Pleistocene iceberg dynamics on the west Svalbard margin: evidence from bathymetric and sub-bottom profiler data

Fang Zhao[a*], Timothy A. Minshull[b*], Anya J. Crocker[b,e], Julian A. Dowdeswell[c], Shiguo Wu[d], Simon M. Soryal[b],

[a] CAS Key Laboratory of Marginal Sea Geology, South China Sea Institute of Oceanology, Chinese Academy of Sciences, Guangzhou 510301, China

[b] Ocean and Earth Science, National Oceanography Centre Southampton, University of Southampton, European Way, Southampton, SO14 3ZH, United Kingdom

[c] Scott Polar Research Institute, University of Cambridge, Cambridge CB2 1ER, United Kingdom

[d] Institute of Deep-Sea Science and Engineering, Chinese Academy of Sciences, Sanya 572000, China

[e] Dept Animal and Plant Sciences, University of Sheffield, Western Bank, Sheffield S10 2TN UK

* zhaofangiocas@gmail.com (Fang Zhao) and tmin@noc.soton.ac.uk (Timothy A. Minshull)

Abstract

Large icebergs leave evidence of their drift via ploughing of the seabed, thereby providing a geological record of episodes of calving from thick ice sheets. We interpret large-scale curvilinear depressions on the western Svalbard margin as ploughmarks produced by the keels of icebergs that grounded on the seafloor as they drifted through this area. Iceberg ploughmarks were identified at modern water depths between 300 m and 1000 m and in two distinct stratigraphic units. Combining data from sediment cores with seismic stratigraphy from sub-bottom profiler data suggests that the ploughmarks developed in two phases: (1) during Marine Isotope Stage (MIS) 6; and (2) during MIS 2, indicating the presence of large drifting icebergs on the western Svalbard margin during both the Late Saalian and Late Weichselian glaciations. Sediment-core data along the western Svalbard margin indicate a sharp increase in mass-transported sediments dated at 23.7 ± 0.2 ka, consistent with the MIS 2 age of the younger iceberg-ploughed surface. The ploughmarks are oriented in two main directions: SW-NE and S-N. S-N oriented ploughmarks, which shallow to the north, indicate iceberg drift from the south with a SW–NE component marking the zone of splitting of the West Spitsbergen Current (WSC) into the Yermak Slope Current (YSC) and North Spitsbergen Current (NSC). Large MIS 6 and MIS 2 icebergs most likely had an Arctic Ocean source. We suggest that these icebergs probably left the Arctic Ocean southward through Fram Strait and circulated within the Norwegian-Greenland Sea before being transported northwards along the Svalbard margin by the WSC. An additional likely source of icebergs to the western Svalbard margin during MIS 2 was the ice-sheet terminating in the western Barents Sea, from which icebergs drifted northward.

Keywords: Icebergs, Iceberg ploughmarks, Western Svalbard margin, West Spitsbergen Current, Pleistocene

1. Introduction

The Fram Strait (Fig. 1) is the only deep water gateway of the Arctic Ocean and, hence, it plays an important role in global ocean circulation and heat exchange (Schauer et al., 2004). The West Spitsbergen Current (WSC) flows along the western Spitsbergen margin on the eastern edge of the Fram Strait, transporting relatively warm, saline waters to the Arctic Ocean, whereas the East Greenland Current (EGC) discharges cold water of relatively low salinity out of the Arctic Ocean along the Greenland margin at the western edge of the Fram Strait. The western Svalbard margin therefore occupies a key position in understanding the exchange of water and ice between the Arctic Ocean and the North Atlantic during the Quaternary. Geological evidence for iceberg activity provides key insights into the temporal variability of glacier-ice export from the Arctic Ocean to the Norwegian-Greenland Sea. Previous studies have suggested that icebergs were present in Fram Strait for much of the Neogene, but their occurrence shows strong temporal variability (e.g. Andersen et al. 1996; Hevrøy et al., 1996, Wolf-Welling et al., 1996), which has been recognized as an important factor influencing global oceanic thermohaline circulation (Aagaard and Carmack, 1989; Bischof and Darby, 1997; Broecker, 2010). Isotopic evidence from Ocean Drilling Program (ODP) Site 910 (Fig. 2a) on the southern Yermak Plateau suggests a strong imprint of Arctic freshwater pulses on the Earth's climate system throughout the last 0.8 Ma (Knies et al., 2007). Sediment-core data from Fram Strait reveal that large quantities of icebergs drifted through the straits into the Greenland Sea several times during the late Pleistocene (Darby et al., 2002), with geophysical evidence from the Hovgaard Ridge revealing very deep (>1200 m) iceberg ploughing (Fig. 1; Arndt et al., 2014; Arndt and Forwick, 2016). It has been suggested, therefore, that large amounts of ice (including giant icebergs) were released from ice shelves in the Arctic Ocean and exported southward through Fram Strait during some glacial maxima (Arndt et al., 2014; Arndt and Forwick, 2016).

In this paper, we present new multibeam bathymetry and sub-bottom profiles from the western Svalbard margin. Our study supports the hypothesis that icebergs sourced in the Arctic Ocean drifted southward through the Fram Strait, then drifted into the Norwegian-Greenland Sea and ploughed the seafloor of the adjacent continental margin driven by ocean currents. In addition, icebergs calved from an ice sheet in the western Barents Sea probably drifted northward to plough the Svalbard margin. We discuss the implications of the observed iceberg grounding for the glacial history and past dynamics of the ice sheet and for the reconstructions of ocean currents.

2. Background: palaeoglaciological, geological and oceanographic setting

It is often suggested that Quaternary Arctic ice sheets terminated at the continental shelf edges in the Arctic (Ehlers and Gibbard, 2007; Svendsen et al., 2004). However, studies over the last few decades have demonstrated that glacier ice may have extended northwards into the deep-sea basins of the Arctic Ocean and/or built up from extensive sea-ice cover during some previous glacial periods (Mercer, 1970; Polyak et al., 2001), particularly during the Saalian, when continental ice sheets were larger than during the more recent Weichselian (Jakobsson et al., 2010, 2016; Niessen et al., 2013). Evidence of ice grounding, which has generally been attributed to ice shelves or giant icebergs, has been identified on the seafloor of the Arctic Ocean down to 1280 m present water depth (Vogt et al., 1994; Polyak et al., 2001; Dowdeswell et al., 2010a; Gebhardt et al., 2011; Jakobsson et al., 2008; Niessen et al., 2013; Arndt and Forwick, 2016; Jakobsson et al., 2016). Glacial landforms such as iceberg ploughmarks, produced by the grounding and ploughing action of deep-keeled icebergs (e.g. Woodworth-Lynas et al., 1985), therefore provide important evidence for past glacial activity in the

Arctic Ocean. Geological and geophysical studies have shown evidence for iceberg ploughmarks on the central Lomonosov Ridge at water depths of up to >1000 m (Fig. 1) (Polyak et al., 2001; Kristoffersen et al., 2004; Jakobsson et al., 2008; Jakobsson et al., 2016) and at similar water depths in the Chukchi Borderland (Jakobsson et al., 2008), on Morris Jesup Rise (Jakobsson et al., 2010) and on the East Siberian continental margin, where they extend as deep as ~1200 m below the present sea level (Niessen et al., 2013). These findings suggest that at least the western Arctic Ocean was covered by a >1000 m thick ice shelf complex during MIS 6 (Jakobsson et al., 2010). The only evidence for major glaciations extending beyond the Eurasian shelf edges is that for the former presence of grounded ice on the Yermak Plateau during MIS 6 (Fig. 1) (Vogt et al., 1994; Dowdeswell et al., 2010a; Gebhardt et al., 2011) and ice grounding on the central Lomonosov Ridge (Jakobsson et al., 2010), as the redeposition of eroded sediments indicates a Eurasian source for the eroding ice (Polyak et al., 2001; Jakobsson et al., 2008). The recently discovered ice-shelf groundings on bathymetric highs in the central Arctic Ocean have a spatially coherent pattern, with grounded ice on the Yermak Plateau, suggesting that an ice shelf extended over the entire central Arctic Ocean during MIS 6 (Jakobsson et al., 2016). The western Barents Sea, through the convergence of ice flow from the former Fennoscandian, Barents Sea and Svalbard ice sheets, also produced fast-flowing ice streams in the Bear Island and Storfjorden troughs (e.g. Ottesen et al., 2005; Andreassen et al., 2008). Ice-sheet grounding in the south-western Barents Sea has been inferred from seismic–reflection data and subglacially produced seafloor landforms imaged in geophysical data, with implications for delivery of ice and sediments from the Barents Sea during the Last Glacial Maximum (e.g. Dowdeswell and Siegert, 1999; Ottesen et al., 2005; Andreassen et al., 2008).

Evidence from geophysical and sediment core data shows that various glacial processes shaped the Svalbard margin during the Quaternary (e.g. Vorren and Laberg, 1997; Butt et al., 2000; Geissler and Jokat, 2004; Ottesen et al., 2005; Dowdeswell et al., 2010a). During the Pleistocene ice ages, ice streams eroded cross-shelf troughs (Batchelor and Dowdeswell, 2014) and sediment transport and deposition resulted in prograding glacigenic sequences on the continental margin (Ottesen et al., 2005, 2007). Glacigenic debris-flows (GDFs) originated during peak glaciations from sediment release along ice stream fronts at the shelf break (e.g. Andersen et al., 1996; Sarkar et al., 2011). The western Svalbard margin is characterized by Late Plio-Pleistocene fan complexes deposited in front of troughs on the continental shelf (Fig. 2a). Their occurrence has been related to ice streams draining westward from ice sheets located over the Barents Sea-Svalbard region (Vorren et al., 1998; Ottesen et al., 2005, 2007). Submarine landforms such as mega-scale glacial lineations, drumlins ,grounding-zone wedges and moraine ridges are identified on the western shelf of Svalbard. They were produced beneath and at the termini of ice sheets retreating onto Svalbard (Ottesen et al., 2007; Dowdeswell et al., 2010b; Dowdeswell et al., 2016). The present-day shelf break marks the maximal glacier expansion on the Svalbard margin (Solheim et al., 1996; Svendsen et al., 2004; Andreassen et al., 2004). Large-scale seafloor ploughmarks produced by deep-keeled icebergs dated at MIS 6 have been observed on the Yermak Plateau. They occur in variable orientations, with predominantly NE and NW trends. These iceberg ploughmarks are interpreted to be produced either by icebergs from a major grounded ice sheet on Svalbard, or by a floating ice-shelf remnant, or by mega-icebergs from the Arctic Basin (Dowdeswell et al., 2010a).

Based on geophysical evidence and data from ODP drill cores (ODP sites 910, 911 and 986, Fig. 2a), it has been suggested that glaciers reached the Svalbard shelf edge several times during the Plio-Pleistocene (Solheim et al., 1996; Shipboard Scientific Party, 1995; Geissler and Jokat, 2004). Mass-transport deposits in the form of glacigenic debris-flows are found on the large trough-mouth fans and, occasionally, in the inter-fans areas, draped with recent hemipelagic sediments (Laberg and Vorren, 1995; Hjelstuen et al., 1996; Andersen et al., 1996; Peersen, 2006; Jessen et al., 2010). The most recent expansion of the Svalbard-Barents Sea Ice Sheet to the shelf edge occurred at approximately 24 ka BP and resulted in instability of the upper slope and the deposition of mass transport deposits along much of the Svalbard margin (Elverhøi et al., 1995; Andersen et al., 1996; Jessen et al., 2010).

The West Spitsbergen Current (WSC) flows northwards along the western margin of Spitsbergen, transporting relatively warm Atlantic Water into the Arctic Ocean (Fig. 2a). To the northwest of Svalbard (c. 80°N), the WSC splits into three branches: the North Spitsbergen Current (NSC) is present where the upper 500 m of surface waters are deflected east by the Coriolis Force to flow to the north of Svalbard; the Yermak Slope Current (YSC) occurs when the remaining deeper waters of the WSC continue to flow north and then east around the northwestern corner of the Yermak Plateau; and the Return Atlantic Current (RAC) is located when the western branch of the WSC turns counterclockwise, eventually returning southward along the eastern edge of the East Greenland Current (Figs. 1-2)

(Manley et al., 1992; Schlichtolz and Houssais, 1999). The WSC is strongly steered by bathymetry, with current velocities along the western Svalbard margin measured at 9 – 16 cm/s between 500 and 1500 m depth, whereas the YSC is slower at 1 – 3 cm/s (Schlichtolz and Houssais, 1999; Fahrbach et al., 2001). Alongslope contour currents are prevalent at high latitudes, due to the influence of the Coriolis Force on steep slopes (Nöst and Isachsen, 2003).

3. Data and methods

In this study, we use swath-bathymetric data and TOPAS sub-bottom profiler data acquired during an International Polar Year project in 2008. The bathymetric survey was performed using a Kongsberg Simrad EM1002 swath-bathymetric system that operated at a frequency of 12 kHz. The survey covered an area of approximately 2500 km^2 spanning water depths of 200 m to 1800 m (Fig. 2b). Bathymetric data were processed using the CARAIBES software through cleaning the navigation data and rejecting incoherent values (Sarkar et al., 2011).

The TOPAS sub-bottom profiler survey track covered ~6000 line-km and spanned a region ~200 km in length and ~10 km in width (Fig. 2b). The TOPAS used a parametric acoustic source which produces a 0.5 – 5.0 kHz, 1 ms chirp signal with energy concentrated at 3 – 4 kHz. The bandwidth and an assumed 1500 m/s sound-velocity through water provides a theoretical vertical resolution of 0.167 m, whereas the theoretical horizontal resolution is dependent upon the depth of the illuminated reflector (Quinn et al., 1998; Schwamborn et al., 2002) and varies between 0.5 m and 3.3 m for our survey. The data were converted to SEG-Y format and processed through the application of a bandpass filter, for removal of frequencies not in the source, chirp correlation, signature deconvolution, instantaneous amplitude, to increase the signal-to-noise ratio. Coherency filtering was also used in order to enhance similar signals in neighbouring traces. The interpretation workflow involved a systematic examination to identify the key seismic horizons with a pick uncertainty of c. 1 ms, and the definition of seismo-stratigraphic units bounded by these horizons. The data were gridded and imaged in IHS Kingdom 8.7 with a grid-cell size of 50 m. We produced isopach maps of these units to understand the spatio-temporal variation of sedimentation, using a flex gridding function.

New and previously published age-depth models and lithological logs from sediment cores, and published seismic stratigraphy from the west Svalbard margin were used to assign ages to the seismic reflectors. Additional age control and sedimentological information were provided by several sediment cores from our study area. In particular, we use three cores taken by the RRS *James Clark Ross* during IPY cruise JR211 in 2008 (JR211-11PC, JR211-13GC and JR211-15GC) and previously published data from sediment cores JM05-030, JM05-031, JM05-032 (Jessen et al., 2010) and MSM5/5-712-2 (Zamelczyk et al., 2014). Magnetic susceptibility data were generated from JR211-13GC using the MSCL-XYZ logger at the British Ocean Sediment Core Research Facility (BOSCORF). This allowed correlation to the magnetic susceptibility stack published by Jessen et al. (2010), with additional constraint provided by lithological comparison, permitting many age tie-points on the Svalbard margin identified by Jessen et al. (2010) to be applied to the chronology of JR211-13GC (suppl. Fig. 1). Elemental ratios of bulk sediment generated by x-ray fluorescence core scanning using the ITRAX^{TM} core scanner at BOSCORF were used to provide correlation of JR211-11PC and JR211-15GC to JR211-13GC (suppl. Fig. 2). New radiocarbon ages of mixed planktonic foraminifera were generated from the JR211 cores by the National Ocean Sciences Accelerator Mass Spectrometry facility (NOSAMS) to provide additional age constraint. All radiocarbon ages (including those previously published) were calibrated using the Calib 7.1 software (Stuiver and Reimer, 1986, http://calib.qub.ac.uk/calib/) in conjunction with the Marine13 calibration curve (Reimer et al. 2013). A reservoir age of 491 ± 35 years was assumed for the calibration of all radiocarbon ages (Mangerud and Gulliksen, 1975; Mangerud, 1972).

4. Morphology of iceberg ploughmarks

4.1 Description

Two groups of curvilinear seafloor depressions are mapped in the study area (Fig. 2b): a more northerly group on the northwestern Svalbard margin (Group I; Fig. 3), and a southerly group, on the western Svalbard margin, south of Kongsfjorden Trough (Group II; Fig. 4). Group I depressions are located in a wide, relatively flat area (average slope approaching 1°) with water depths < 1000 m at the resolution of our swath imagery (Fig. 3a). Seventeen elongate curvilinear features which form Group I are identified in the bathymetric data at water depths between 500 and 980 m (Figs. 3 and 5a), with lengths of 3.3 km to 15 km, widths of 408 m to 1700 m and depths of 5.9 m to 37 m (Fig. 5c-e). The curvilinear features occur in two main orientations. Five of them (P1, P2, P13, P14 and P15) are oriented in a north-south direction (S-N/N-S) with grid bearing of ~170° to 180° (Figs. 3, 5b). The orientation of the other depressions on the northwestern Svalbard margin is predominantly SW-NE, with grid bearing ranging from 200° to 260°. The depth of these depressions decreases from southwest to northeast (Fig. 3d). Some of the large depressions are parallel to each other (e.g. P1,P2 and P13; P5, P7, P11 and P16; P14 and P15), whereas others with the same general orientation are not parallel, with grid-bearings differences of up to 60° (Figs. 3 and 5). The depressions of similar orientations are parallel to sub-parallel for distances of many kilometres. In the sub-bottom profiles, the shallow stratigraphy is characterized by single irregular V-shaped (P2, P3, P5, P10, P11, P16) and W-shaped (P1, P6, P7, P8) depressions covered by ~2-18 m of well-stratified sediments (assuming an interval velocity of 1500 m/s) (Figs. 6-7). These features are mostly around 20 m deep relative to the surrounding seafloor but can be up to 27 m deep. The sedimentary cover becomes slightly thinner closer towards the upper slope (Fig. 7).

Thirty-one curvilinear depressions of Group II are identified on the western Svalbard margin, in water depths between 395 and 860 m (Figs. 4, 5a). The slope here is steeper, with slope angles of ~ 1.2°-2.0°. The depressions have lengths of 1.3 km to 5.6 km, widths of 105 m to 470 m and depths of 1.5 m to 11 m (Fig. 5c-e). The orientation of the depressions is predominantly S-N but varies by up to 40° (Figs. 4, 5b). The shallow stratigraphy of the western Svalbard margin is characterised by parallel undulating reflectors (Fig. 8). Most of the ploughmarks in deeper water are longer, wider and deeper than those in shallower water. Overall, the iceberg ploughmarks in Group I are larger than those in Group Ⅱ. In addition, the seafloor is generally much smoother on the northwestern Svalbard margin than on the western margin, with considerably more distinct depressions.

4.2 Interpretation

The curvilinear depressions on the western Svalbard margin are of similar morphology to various linear to curvilinear submarine landforms described on both Arctic and Antarctic continental shelves that are interpreted to have been formed as a result of ploughing of the seafloor by iceberg keels (e.g. Barnes and Lien, 1988; Dowdeswell et al., 1993; Dowdeswell et al., 2010a). We identified such ploughmarks using the approach of Pudsey et al. (1994) and Graham et al. (2009). Specifically, we selected straight to sinuous furrows. Ploughmark identification was limited by the resolution of our dataset, and we did not classify features as ploughmarks unless we had a high degree of confidence in the identification, so some fainter ploughmarks may be missed.

The occurrence of erosive ploughmarks on the northwestern and western Svalbard margin suggests that megabergs or ice-shelf remnants have drifted across the seafloor. The sets of parallel ploughmarks have probably been produced by multiple keels of a single megaberg or by the keels of several icebergs that were trapped together in huge multi-year sea ice floes (Kristoffersen et al., 2004; Graham et al., 2009). Other ploughmarks that are not parallel to one another were probably formed by keels of several individual giant icebergs rather than by a single multikeeled iceberg (Figs. 3 and 4).

The two orientations of large ploughmarks in Group I indicate that the icebergs may have come from two different directions (Fig. 5b). Cross-cutting relationships can be seen amongst the ploughmarks, with, for example, P3 covered by the ridges of P1, indicating that P3 developed earlier than P1 (Fig. 3c). The ploughmarks decrease in water depth from southwest to northeast, indicating that icebergs ploughed the palaeo-seafloor while travelling in a northeasterly direction (Fig. 3d). The water depth of iceberg ploughmarks oriented in a S-N direction in the two groups shows less variation. Therefore we cannot determine whether these icebergs travelled from south to north or north to south from bathymetric data alone.

5. Acoustic stratigraphy of the northwestern and western Svalbard margin

5.1 Description

We identified three seismic reflectors – L1 (youngest) to L3 (oldest) that could be traced across our survey area, defining three acoustic units from the shallow stratigraphy (Figs. 6-8; Table 1). Reflector L1 (red) marks a shallow erosional surface (Figs. 6-8). The horizons below L1 only truncate against L1 on the western Svalbard margin and not on the northwestern margin (Fig. 8). L2 (blue) marks the top of the underlying transparent package (Unit 2; Figs. 6-7). L3 (purple) marks a deep erosional surface, which forms the base of the northwestern group of iceberg ploughmarks (Fig. 6-7).

Isopach maps for Subunit 1A, Subunit 1B and Unit 2 reveal the changes in sediment thickness above L3 on the western Svalbard margin (Fig. 9). The isopachs exhibit similar variations in sediment thickness between the upper and lower slope, with the thickest sediment packages generally found at greater water depths. Isopach maps show a depocentre at the mouth of Kongsfjorden cross-shelf trough and a much deeper elliptical depocentre close to the Molloy Ridge (Fig. 9). Between these two depocentres, Units 1 and 2 are thin. On the northwestern corner of the Svalbard margin, the isopach maps display apparent linear or patchy structures with higher sediment thickness at the locations of the ploughmarks on the slope (Fig. 9).

5.2 Interpretation

The truncations of L1 and L3 reflectors show that the ploughmarks are produced by erosion (Figs. 6–8). We therefore infer that L1 and L3 represent palaeo-seafloors that were ploughed by icebergs and then draped by the overlying stratified sediment. The large variations in sediment thickness between the upper slope and lower slope suggest that the lower slope marks a transition between depositional environments (Fig. 9). Thicker areas of Units 1 and 2 are observed at the mouth of Kongsfjorden cross-shelf trough and on the lower slope of the northwest and west Svalbard margin. It has been suggested that the mouth of Kongsfjorden Trough is the location of extensive progradation and fan development (Sarkar et al., 2011). The deeper elliptical depocentre was likely formed by the NSC where the upper 500 m of surface waters were deflected east and flowed to the north of Svalbard and generated contourite deposits possibly related to a drop in current velocity. The linear or patchy structures with higher sediment thickness on the northwestern corner of the Svalbard margin suggest that greater sediment infilling may have taken place in some of the iceberg ploughmarks on the slope where the NSC flowed at shallower depths.

6. Age of the iceberg ploughmarks on the northwestern and western Svalbard margin

To provide chronological control on the acoustic stratigraphy outlined above, we use data from three new (JR211-11PC, JR211-13GC, JR211-15GC) and four existing (JM05-030, JM05-031, JM05-032 and MSM5/5-712-2) short piston and gravity cores collected from 78° to 80°N along the western Svalbard margin (Fig. 2b; Jessen et al., 2010; Zamelczyk et al., 2014). Six of these cores fall within the Group I or II regions, with two occurring particularly close to the iceberg ploughmarks identified here (JM05-031, JM05-032). Age models suggest that all seven cores reach MIS 2 (Fig. 10; Jessen et al., 2010; Zamelczyk et al., 2014), with the three new cores (JR211-11PC, JR211-13GC, JR211-15GC) extending back into MIS 3 (Fig. 10). One feature preserved in all seven cores is a prominent interval characterised by coarse, poorly sorted sediments, commonly dark in colour, with low magnetic susceptibility. These sediments have been interpreted as mass transport deposits related to the expansion of the Svalbard-Barents Ice Sheet to the edge of the western Svalbard shelf, and have been dated at 23,150 ± 200 – 23,670 ± 190 years BP (Jessen et al., 2010). They are identified in the new sediment cores at depths of 147.5 – 171.5 cm (JR211-11PC), 220 – 234.5 cm (JR211-13GC), and 40 – 75.5 cm (JR211-15GC). Little sediment is recovered above the mass transport deposits in cores

JR211-15GC and JR211-11PC. This could potentially be a result of the top of the sediment not being captured by the coring process; however, similar radiocarbon-derived core-top ages recorded in nearby sites JM05-032, JM05-031 (Jessen et al., 2010) and JR211-16GC (unpublished data) suggest that the absence of younger sediment is more likely to be the result of erosion or an interval of non/minimal deposition. In particular, very condensed to no sedimentation observed at the up-slope sides of iceberg ploughmarks might be current induced.

An acoustic velocity of 1500 m/s was used to convert the depth values to vertical intervals in two-way travel time, and enable correlation with the seismic profiles (and vice versa). In this way, reflector L1 can be approximately dated at about 24 kyr. The estimated depth of this reflector is in good agreement with the depth of the mass transport deposits in nearby sediment cores, and the reflector marks the base of a thin transparent zone consistent with such deposits. This observation suggests that iceberg-produced features in Group Ⅱ on the western Svalbard margin most likely occurred at or around MIS 2, when the ice reached the shelf edge at maximum glacial state. A lack of core ages within our survey area prevents direct dating of deeper reflectors. A regional reflector, A3, which matches closely the slope reflector R3 (~126 m depth below seafloor at ODP Site 986) in seismic line NP 90-303 (see location in Fig. 2b), is dated at ~780 kyr (Elverhøi et al., 1995; Forsberg et al., 1999; Butt et al., 2000; Sarkar et al., 2011). We used the two dated horizons (A3, L1) to estimate the age of L3 by assuming a constant sedimentation rate between L1 and L3. This approach is clearly an approximation because the rate is likely to vary greatly between glacial and interglacial periods, but the rate will be dominated by the glacial periods. Evidence from shallow cores suggests that within the last glacial period, sedimentation rates vary between sites but are roughly constant at each site (Fig. 10). Analysis of a slope-parallel seismic profile (JR211-21) identified reflector A3 at ~46 ms beneath the seafloor, around core sites JM05-031 and JM05-032 (Fig. 7c). Here L1 occurs at 8 ms beneath the seafloor and L3 at 16 ms. The P-wave velocities determined by Chabert et al. (2011) are c. 1542 m/s for the interval between L1 and L3, and c. 1684 m/s for the interval between L3 and A3. Thus L1 is at 6 m depth, L3 is at 12 m, A3 is at 37 m and, hence, the age of L3 can be estimated as c. 147 ka. This age indicates that the northwestern group of ploughmarks was formed during MIS 6 (c. 185-135 ka), coincident with a major ice grounding event during MIS 6 in the Arctic Ocean (Jakobsson et al., 2010). The thick transparent unit above L3 may also represent mass transport deposits, but we have no core data to support this interpretation.

7. Source regions for icebergs on the western Svalbard margin

Our age estimates for reflectors L1 and L3 lead us to propose that the observed iceberg ploughmarks on the northwestern (Group I) and western Svalbard (Group II) margin were formed during MIS 6 and MIS 2, respectively. The MIS 6 age matches that inferred for deep-keeled icebergs elsewhere in the Arctic (Figs. 1, 11; Jakobsson, 1999; Jakobsson et al., 2016; Polyak et al., 2001; Jakobsson et al., 2010; Dowdeswell et al., 2010a; Arndt et al., 2014). There is little evidence to suggest ice-grounding on the Lomonosov Ridge, Morris Jessup Rise or Yermak Plateau during MIS 2. However, evidence for ice-rafting of debris during MIS 2 from the Laurentide, Innuitian and Barents–Kara Ice Sheets has been found in Arctic Ocean cores (Darby and Zimmerman, 2008; Mangerud et al., 1998; Svendsen et al., 2004). Within the Pleistocene, the transport of ice from the Arctic Ocean into the Norwegian-Greenland Sea via Fram Strait has been documented by several previous studies, based on geophysical data and on abundant ice-rafted debris (IRD) and coal fragments in long sediment cores (Darby et al., 2002; Darby and Zimmerman, 2008; Wollenburg, 2012; Arndt er al., 2014). It is possible, therefore, that icebergs from the Arctic Ocean may have reached the northwestern and western Svalbard margin.

Theoretical analyses indicate that the deepest ploughmarks can be deeper than the thickness of the ice margins calving the icebergs, because unusual overturning events can increase iceberg draft by up to 50% (Lewis and Bennett, 1984; Barnes and Lien,1988). Our multibeam data reveal ploughmarks reaching ~395 – 980 m at present water depth. Assuming a 120 m lower sea level under full-glacial conditions (Rohling et al., 2009), and neglecting isostatic loading effects, the iceberg drafts are estimated to range from 275 m to 860 m. Therefore, the minimum thickness of ice sheets that calved icebergs into relatively deep water was ~180 m for calving the shallowest iceberg and ~570 m for the deepest iceberg.

Based on the locations of high Arctic cross-shelf troughs provided by Batchelor and Dowdeswell (2014), likely sources for deep-keeled icebergs around the Arctic Ocean are ice streams that occupied deep troughs in Southern Greenland, Baffin Bay, the Queen Elizabeth Islands, the Canadian Arctic Archipelago, the Beaufort Sea Shelf and the northern Barents-Kara during full-glacial periods (Fig. 12). Several large glacial troughs extending across the Queen Elizabeth Islands, Canadian Arctic Archipelago and the Beaufort Sea Shelf, e.g. M’Clintock Inlet, have been carved by primary ice streams discharging directly into the Arctic Ocean from the Laurentide and Innuitian ice sheets (Fig. 12; England et al., 2009; Jakobsson et al. 2014). The fast-flowing ice streams in the Franz Victoria and St. Anna troughs that flowed into the Arctic Ocean from the northern part of the Barents Sea also provide likely sources for giant icebergs (Fig. 12; Vogt et al., 1994; Kleiber et al., 2000; Svendsen et al., 2004; Dowdeswell et al., 2010a). Similar giant iceberg ploughmarks at depths of up to 1200 m have been observed along the East Siberian continental margin (Niessen et al., 2013). However, in order to be transported to the Fram Strait, such large icebergs from the East Siberian continental margin need to cross the Lomonosov Ridge, which has only a few deep gateways.

There are also potential iceberg source regions south of the Arctic Ocean. Evidence for relatively thick grounded ice is present in the Bear Island Trough, which may have been the source of icebergs with a keel depth of up to about 500 m (Andreassen et al., 2008; Batchelor and Dowdeswell, 2014). Southern Greenland and Baffin Bay can be excluded as source areas, since very large icebergs from these sources cannot reach the west Svalbard margin due to shallow bathymetric obstacles in the North Atlantic (<700 m at Denmark Strait). Svalbard itself can also be excluded as a source area due to relatively shallow water depths (< 400 m) in the cross-shelf troughs which prevents the formation of icebergs with suffiently deep keels. Therefore, we suggest that the Arctic Ocean is the most likely source for the giant MIS 2 and MIS 6 icebergs which reached the western Spitsbergen margin, with smaller icebergs in Group II also sourced from the Western Barents Sea (Fig. 12).

Icebergs are mainly steered by ocean currents, and to a lesser extent by wind and waves (Death et al., 2006). There are two possible routes for the arrival of icebergs on the northwestern and western Svalbard margin (Fig. 12b). The first route involves icebergs travelling from the Arctic Ocean through Fram Strait and circulating within the Norwegian-Greenland Sea, before becoming grounded on the northwestern Svalbard margin (Fig. 12b). This route is consistent with geophysical evidence of ice grounding on the Hovgaard Ridge, dated as MIS 6 with N-S oriented ploughmarks indicating the southward passage of icebergs through the Fram Strait (Arndt et al., 2014; Arndt and Forwick, 2016; Fig. 11). The other route, for smaller icebergs (<500 m), involves northward travel from the Bear Island Trough in the West Spitsbergen Current (Fig. 12b). The fine-fraction material from sediment cores on the NW continental margin of Svalbard and the Yermak Plateau supports the idea of northward transport of this material along the western Svalbard continental slope from the advanced Barents Sea Ice Sheet (Vogt et al., 2001). Therefore, a large amount of ice was likely exported to high latitudes by the WSC. We propose that Bear Island ice stream-derived icebergs were delivered to the western Svalbard margin and ploughed the palaeo-seafloor during MIS 2.

Evidence from the northwestern Svalbard margin shows the modification of iceberg transport directions by branches of the WSC (Fig. 12b). Twelve iceberg ploughmarks of Group Ⅰ oriented in NW-SE direction correspond to the flow direction of the NSC. Another five ploughmarks in a S-N direction are consistent with the flow direction of the YSC. Further south, the iceberg ploughmarks in Group Ⅱ are oriented south to north, corresponding to the flow direction of WSC (which is the dominant current along the western Spitsbergen margin). The ploughmarks therefore show strong evidence of the three different ocean currents - WSC, NSC and YSC - on the Svalbard margin. This suggests that these three currents persisted with significant vigour during peak glacial conditions.

8. Conclusions

From an analysis of swath-bathymetric, sub-bottom profiler and shallow sediment core data, we conclude the following.

1. Within the Pleistocene sediments of the Svalbard margin, two groups of linear to curvilinear depressions are present in water depths of 300 m to 1000 m, interpreted as ploughmarks produced by the keels of icebergs during previous periods of ice-rafting on high-latitude continental shelves. Seventeen ploughmarks of Group Ⅰ are located on the northwest Svalbard margin in water as deep as 980 m and oriented in NE-SW and N-S directions (Fig. 3). The 31 ploughmarks in Group Ⅱ on the western Svalbard margin are observed down to ~ 860 m present water depth, and are oriented in a N-S direction (Fig. 4). Most ploughmarks in Group Ⅰ are much larger than those in Group Ⅱ. The iceberg ploughmarks of the western Svalbard margin are very similar in size, but quite different in pattern to swath images of iceberg ploughmarks from the Yermak Plateau (Fig. 11). We infer that they were not produced by icebergs from the Yermak Plateau.
2. Dating of sediment cores combined with published stratigraphic observations suggests that the iceberg ploughmarks on the western Svalbard margin were formed in two stages: those in Group Ⅰ developed at or around MIS 6, corresponding to a major ice growth and grounding event in the Arctic Ocean. The iceberg ploughmarks in Group Ⅱ occurred at or around MIS 2 and were related to late Weichselian glaciation. Furthermore, the age model inferred in the cores located in water depths between 500 and 1500 m along the western Svalbard margin implies that a discrete interval

of mass-transport deposits with iceberg erosional structures is related to ice-grounding events that occurred at c. 24 ka. The two groups of iceberg ploughmarks indicate the presence of drifting mega-icebergs on the northwest and western Svalbard margin in MIS 6 and MIS 2, respectively.

Our study suggests that the iceberg sources were probably MIS 6 and MIS 2 ice streams within Saalian and Weichselian ice sheets (Fig. 12). The predominantly S-N trend of ploughmarks indicates that icebergs drifted along the west Svalbard margin from south to north steered by the WSC. On the northwestern part of the margin, the SW-NE orientation of some of the ploughmarks indicates the zone of splitting of the WSC into the YSC and NSC, suggesting that icebergs of distant origin may have been transported by ocean currents in similar directions. We suggest that the largest icebergs were originally released into the Arctic Ocean before travelling southward through the Fram Strait, circulating within the Norwegian-Greenland Sea and then drifting northwards along the Svalbard margin in the WSC during MIS 6 and MIS 2. Another potential origin for the relatively smaller MIS 2 ploughmarks is proposed that icebergs were released from the western Barents Sea and transported directly northward.

Acknowledgements

We acknowledge University of Southampton, the China Scholarship Council and the National Natural Science Foundation of China (Nos. 91328206 and 41576041) for supporting F.Z.'s research. Data acquisition was supported by the UK Natural Environment Research Council as part of the International Polar Year 2007-2008 “Dynamics of gas hydrates in polar marine environments” (grant number NE/D005728). We thank Principal Scientist Graham Westbrook and the captain, crew and scientific party of cruise JR211 for their hard work at sea. We are also grateful to the staff at BOSCORF and NOSAMS for their assistance in generating sediment core data. The editor Henning A. Bauch and three anonymous reviewers are acknowledged for their helpful reviews.

References

Aagaard, K., Carmack, E.C., 1989. The role of sea ice and other fresh water in the Arctic circulation. J. Geophys. Res. 94, 14, 485–14,498, doi:10.1029/JC094iC10p14485.

Andersen, E.S., Dokken, T.M., Elverhøi, A., Solheim, A., Fossen, I., 1996. Late Quaternary sedimentation and glacial history of the western Svalbard continental margin. Mar. Geol. 133, 123-156.

Andreassen, K., Nilssen, L.C., Rafaelsen, B., Kuilman, L., 2004. Three-dimensional seismic data from the Barents Sea margin reveal evidence of past ice streams and their dynamics. Geology 32, 729–732.

Andreassen, K., Laberg, J.S., Vorren, T. O., 2008. Seafloor geomorphology of the SW Barents Sea and its glaci-dynamic implications. Geomorphology 97, 157–177.

Andreassen, K., Winsborrow, M., Bjarnadóttir, L. R., and Rüther, D. C., 2014. Ice stream retreat dynamics inferred from an assemblage of landforms in the northern Barents Sea. Quat. Sci. Rev. 92, 246–257.

Arndt, J.E., Forwick, M., 2016. Deep-water iceberg ploughmarks on Hovgaard Ridge, Fram Strait. In, In Dowdeswell, J.A., Canals, M., Jakobsson, M., Todd, B.J., Dowdeswell, E.K. and Hogan, K.A., (eds), Atlas of Submarine Glacial Landforms: Modern, Quaternary and Ancient. Geological Society, London, Memoirs 46, 285-286.

Arndt, J.E., Niessen, F., Jokat, J., Dorschel, B., 2014. Deep water paleo-iceberg scouring on top of Hovgaard Ridge–Arctic Ocean. Geophys. Res. Lett. 41, 5068–5074, doi:10.1002/2014GL060267.

Barnes, P.W., Lien, R., 1988. Icebergs rework shelf sediments to 500 m off Antarctica. Geology 16, 1130-1133.

Batchelor, C.L., Dowdeswell, J.A., 2014. The physiography of High Arctic cross-shelf troughs. Quat. Sci. Rev. 92, 68–96, doi:10.1016/j.quascirev.2013.05.025.

Broecker, W. S., 2010. The Great Ocean Conveyor: Discovering the Trigger for Abrupt Climate Change, 176, Princeton Univ. Press, Princeton.

Bischof, J. F., Darby, D. A., 1997. Mid to late Pleistocene ice drift in the western Arctic Ocean: Evidence for a different circulation in the past. Science 277, 74 – 78.

Butt, F.A., Elverhøi, A., Solheim, A., Forsberg, C.F., 2000. Deciphering late Cenozoic development of the western Svalbard margin from ODP site 986 results. Mar. Geol. 169, 373-390.

Darby, D.A., Bischof, J.F., Spielhagen, R.F., Marshall, S.A., Herman, S.W., 2002. Arctic ice export events and their potential impact on global climate during the late Pleistocene, Paleoceanography 17, 1025, doi:10.1029/2001pa000639.

Darby, D.A., Zimmerman, P., 2008. Ice-rafted detritus events in the arctic during the last glacial interval and the timing of the Innuitian and Laurentide ice sheet calving events. Polar Res. 27, 114-127.

Death, R., Siegert, M.J., Bigg, G.R., Wadley, M.R., 2006. Modelling iceberg trajectories, sedimentation rates and meltwater input to the ocean from the Eurasian Ice Sheet at the Last Glacial Maximum.

Palaeogeogr. Palaeoclimatol. Palaeoecol. 236, 135–150, doi:10.1016/j.palaeo.2005.11.040.

Dowdeswell, J.A., Bamber, J.L., 2007. Keel depths of modern Antarctic icebergs and implications for sea-floor scouring in the geological record. Mar. Geol. 243, 120–131, doi:10.1016/j.margeo.2007.04.008

Dowdeswell, J.A. and Siegert, M.J., 1999. Ice-sheet numerical modeling and marine geophysical measurements of glacier-derived sedimentation on the Eurasian Arctic continental margins. Geological Society of America Bulletin 111, 1080-1097.

Dowdeswell, J.A., Villinger, H., Whittington, R.J. and Marienfeld, P., 1993. Iceberg scouring in Scoresby Sund and on the East Greenland continental shelf. Mar. Geol. 111, 37-53.

Dowdeswell, J.A., Jakobsson, M., Hogan, K.A., O'Regan, M., Backman, J., Evans, J., Hell, B., Löwemark, L., Marcussen, C., Noormets, R., Ó Cofaigh, C., Sellen, E., Sölvsten, M., 2010a. High-resolution geophysical observations of the Yermak Plateau and northern Svalbard margin: Implications for ice-sheet grounding and deep-keeled icebergs. Quat. Sci. Rev. 29, 3518–3531, doi:10.1016/j.quascirev.2010.06.002.

Dowdeswell, J.A., Hogan, K.A., Evans, J., Noormets, R., Ó Cofaigh, C., Ottesen, D., 2010b. Past ice-sheet flow east of Svalbard inferred from streamlined subglacial landforms. Geology 38, 163-166.

Ehlers, J., Gibbard, P. L., 2007. The extent and chronology of Cenozoic Global Glaciation. Quatern. Int. 164-165, 6-20.

Dowdeswell, J.A., Ottesen, D., Forwick, M., 2016. Grounding-zone wedges on the western Svalbard shelf. In Dowdeswell, J.A., Canals, M., Jakobsson, M., Todd, B.J., Dowdeswell, E.K., Hogan, K.A., (eds), Atlas of Submarine Glacial Landforms: Modern, Quaternary and Ancient. Geological Society, London, Memoirs 46, 233-234.

Eiken, O., Hinz, K., 1993. Contourites in the Fram Strait. Sedimentary Geology 82, 15-32.

Elverhøi, A., Svendsen, J.I., Solheim, A., Andersen, E.S., Milliman, J., Mangerud, J., Hooke, R.L., 1995. Late Quaternary sediment yield from the High Arctic Svalbard area. J. Geol. 103, 1-17.

England, J.H., Furze, M.F.A., Doupe', J.P., 2009. Revision of the NW Laurentide Ice Sheet: implications for paleoclimate, the northeast extremity of Beringia, and Arctic Ocean sedimentation. Quat. Sci. Rev. 28, 1573-1596.

Fahrbach, E., Meincke, J., Osterhus, S., Rohardt, G., Schauer, U., Tverberg, V.andVerduin, J., 2001. Direct measurements of volume transports through Fram Strait. Polar Res. 20, 217–224.

Flower, B.P., 1997. Overconsolidated section on the Yermak Plateau, Arctic Ocean: ice sheet grounding prior to 660 ka? Geology 25, 147-150.

Forsberg, C.F., Solheim, A., Elverhøi, A., Jansen, E., Channell, J.E.T., Andersen, E.S., 1999. The depositional environment of the western Svalbard margin during the upper Pliocene and the Pleistocene; sedimentary facies changes at Site 986. In: Raymo, M.E., Jansen, E., Blum, P., Herbert, T.D. (Eds.), Proceedings of the Ocean Drilling Program. Scientific Results, Leg 162. Ocean Drilling Program, College Station, Texas, 233-246.

Gebhardt, A.C., Jokat, W., Niessen, F., Matthiessen, J., Geissler, W.H., Schenke, H.W., 2011. Ice sheet grounding and iceberg plow marks on the northern and central Yermak Plateau revealed by geophysical data. Quat. Sci. Rev. 30, 1726-1738.

Geissler, W.H., Jokat, W., 2004. A geophysical study of the northern Svalbard continental margin. Geophys. J. Int. 158, 50-66.

Graham, A. G. C., Larter, R. D., Gohl, K., Hillenbrand, C.-D., Smith, J.A., Kuhn, G., 2009. Bedform signature of a West Antarctic palaeo-ice stream reveals a multi-temporal record of flow and substrate control. Quat. Sci. Rev. 28, 2774–2793, doi:10.1016/j.quascirev.2009.07.003

Grosswald, M.G., Hughes, T.J., 2008. The case for an ice shelf in the Pleistocene Arctic Ocean. Polar Geogr. 31, 69-78.

Hjelstuen, B.O., Elverhøi, A., Falaide, J.I., 1996. Cenozoic erosion and sediment yield in the drainage area of the Storfjorden Fan. Global Planet. Change 12, 95-117.

Hughes, T.J., Denton, G.H., Grosswald, M.G., 1977. Was there a late-Würm Arctic ice sheet? Nature 266, 596-602.

Jakobsson, M., 1999. First high-resolution chirp sonar profiles from the central Arctic Ocean reveal erosion of Lomonsov Ridge sediments. Mar. Geol. 158, 111-123.

Jakobsson, M., Polyak, L., Edwards, M., Kleman, J., Coakley, B., 2008. Glacial geomorphology of the Central Arctic Ocean: the Chukchi Borderland and the Lomonosov Ridge. Earth Surf. Proc. Land. 33, 526-545.

Jakobsson, M., Nilsson, J., O'Regan, M., Backman, J., Löwemark, L., Dowdeswell, J.A., Mayer, L., Polyak, L., Colleoni, F., Anderson, L.G., Björk, G., Darby, D., Eriksson, B., Hanslik, D., Hell, B., Marcussen, C., Sellén, E., Wallin, Å., 2010. An Arctic Ocean ice shelf during MIS 6 constrained by new geophysical and geological data. Quat. Sci. Rev. 29, 3505-3517.

Jakobsson, M., Andreassen, K., Bjarnadóttir, L.R., Dove, D., Dowdeswell, J.A., England, J.H., Funder, S., Hogan, K., Ingólfsson, Ó., Jennings, A., Krog Larsen, N., Kirchner, N., Landvik, J.Y., Mayer, L., Mikkelsen, N., Möller, P., Niessen, F., Nilsson, J., O'Regan, M., Polyak, L., Nørgaard-Pedersen, N., Stein, R., 2014. Arctic Ocean glacial history. Quat. Sci. Rev. 92, 40-67.

Jakobsson, M., Nilsson, J., Anderson, L., Backman, J., Bjork, G., Cronin, T.M., Kirchner, N., Koshurnikov, A., Mayer, L., Noormets, R., O/'Regan, M., Stranne, C., Ananiev, R., Barrientos Macho, N., Cherniykh, D., Coxall, H., Eriksson, B., Floden, T., Gemery, L., Gustafsson, O., Jerram, K., Johansson, C., Khortov, A., Mohammad, R., Semiletov, I., 2016. Evidence for an ice shelf covering the central Arctic Ocean during the penultimate glaciation. Nat Commun 7, doi: 10.1038/ncomms10365.

Jessen, S.P., Rasmussen, T.L., Nielsen, T., Solheim, A., 2010. A new Late Weichselian and Holocene marine chronology for the western Svalbard slope 30,000-0 cal years BP. Quat. Sci. Rev., 29, 1301–1312, doi:10.1016/j.quascirev.2010.02.020.

Kleiber, H.P., Knies, J., Niessen, F., 2000. The Late Weichsalian glaciation of the Franz Victoria Trough, northern Barents Sea: ice sheet extent and timing. Mar. Geol. 168, 25-44.

Knies, J., Matthiessen, J., Mackensen, A., Stein, R., Vogt, C., Frederichs, T., Nam, S.-I., 2007. Effects of Arctic freshwater forcing on thermohaline circulation during the Pleistocene. Geology 35, 1075–1078, doi:10.1130/g23966a.1

Kristoffersen, Y., Coakley, B., Jokat, W., Edwards, M., Brekke, H., Gjengedal, J., 2004. Seabed erosion on the Lomonosov Ridge, central Arctic Ocean: a tale of deep draft icebergs in the Eurasia Basin and the influence of Atlantic water inflow on iceberg motion? Paleoceanography 19, PA3006. doi:10.1029/2003PA000985.

Laberg, J.S., Vorren, T.O., 1995. Late Weichselian submarine debris flow deposits on the Bear Island Trough Mouth Fan. Mar. Geol. 127, 45-72.

Lewis, J.C., Bennett, G., 1984. Monte Carlo calculations of iceberg draft changes caused by rolls. Cold Reg. Sci. Techol. 10, 1-10.

Lisiecki, L.E., Raymo, M.E., 2005. A Pliocene-Pleistocene stack of 57 globally distributed benthic $\delta^{18}O$ records. Paleoceanography 20, 1-17, doi: 10.10292004PA001071.

Lloyd, J.M., Kroon, D., Boulton, G.S., Laban, C., Fallick, A., 1996. Ice rafting history from the Spitsbergen ice cap over the last 200 kyr. Mar. Geol. 131, 103-121.

Polyak, L., Edwards, M.H., Coakley, B.J., Jakobsson, M., 2001. Ice shelves in the Pleistocene Arctic

Ocean inferred from glaciogenic deep-sea bedforms. Nature 410, 453-457.

Mangerud, J. 1972. Radiocarbon dating of marine shells, including a discussion of apparent age of Recent shells from Norway. Boreas 1, 143-172.

Mangerud, J., Gulliksen, S., 1975. Apparent radiocarbon ages of recent marine shells from Norway, Spitsbergen, and Arctic Canada. Quat. Res. 5, 263-273.

Mangerud, J., Dokken, T., Hebbeln, D., Heggen, B., Ingólfsson, O., Landvik, J.Y., Mejdahl, V., Svendsen, J.I., Vorren, T.O., 1998. Fluctuations of the Svalbard-Barents Sea ice sheet during the last 150000 years. Quat. Sci. Rev. 17, 11-42.

Manley, T.O., Bourke, R.H., Hunkins, K.L., 1992. Near-surface circulation over the Yermak plateau in northern Fram Strait. J. Marine Syst. 3, 107-125.

Mercer, J.H., 1970. A former ice sheet in the Arctic Ocean. Palaeogeogr. Palaeoclimatol. Palaeoecol. 8, 19-27.

Niessen, F., et al. 2013, Repeated Pleistocene glaciation of the East Siberian continental margin, Nat. Geosci. 6(10), 842–846, doi:10.1038/ngeo1904.

Nöst, O.A., Isachsen, P.E., 2003. The large-scale time-mean ocean circulation in the Nordic Seas and Arctic Ocean estimated from simplified dynamics. J. Mar. Res. 61,175–210.

Ottesen, D., Dowdeswell, J.A., 2009. An inter-ice stream glaciated margin: submarine landforms and a geomorphic model based on marine-geophysical data from Svalbard. Geol. Soc. Am. Bull. 121, 1647-1665. doi:10.1130/B26467.1.

Ottesen, D., Dowdeswell, J.A., Rise, L., 2005. Submarine landforms and the reconstruction of fast-flowing ice streams within a large Quaternary ice sheet: the 2500 km-long Norwegian-Svalbard margin (57-80N). Geol. Soc. Am. Bull. 117, 1033-1050.

Ottesen, D.A.G., Dowdeswell, J.A., Landvik, J.Y., Mienert, J., 2007. Dynamics of the Late Weichselian ice sheet on Svalbard inferred from high-resolution sea-floor morphology. Boreas 36, 286-306.

Peersen, R., 2006. Sedimentary processes on the Svalbard-Barents Sea continental margin and glacial history of the Storfjorden area from the LGM through the Early Holocene. Unpublished Master thesis, Department of Earth Science, University of Bergen, Norway.

Polyak, L., Forman, S.L., Herlihy, F.A., Ivanov, G., Krinitsky, P., 1997. Late Weichselian deglacial history of the Svyataya (Saint) Anna Trough, northern Kara Sea, Arctic Russia. Mar. Geol. 143, 169–188, doi:10.1016/S0025-3227(97)00096-0.

Polyak, L., Edwards, M., Coakley, B., Jakobsson, M., 2001. Ice shelves in the Pleistocene Arctic Ocean inferred from glacigenic deep-sea bedforms. Nature 410, 453-457.

Pudsey, C.J., Barker, P.F., Larter, R.D., 1994. Ice sheet retreat from the Antarctic Peninsula shelf. Continental Shelf Research 14, 1647–1675, doi:10.1016/0278-4343(94)90041-8.

Quinn, R., Bull, J.M., Dix, J.K., 1998. Optimal Processing of Marine High-Resolution Seismic Reflection (Chirp) Data, Mar. Geophys. Res. 20, 13-20.

Sarkar, S., Berndt, C., Chabert, A., Masson, D.G., Minshull, T.A., Westbrook, G.K., 2011. Switching of a paleo-ice stream in northwest Svalbard. Quat. Sci. Rev. 30, 1710-1725.

Schauer, U., Fahrbach, E., Osterhus, S., Rohardt, G., 2004. Arctic warming through the Fram Strait: Oceanic heat transport from 3 years of measurements. J. Geophys. Res. 109, C06026, doi:10.1029/2003jc001823.

Schlichtolz, P., Houssais, M.-N., 1999. An inverse modelling study in Fram Strait. Part I: dynamics and circulation. Deep-Sea Res. II 46, 1083–1135.

Schwamborn, G.J., Dix, J.K., Bull, J.M., Rachold, V., 2002. High-resolution seismic and ground penetrating radar-geophysical profiling of a thermokarst lake in the western Lena Delta, Northern Siberia, Permafrost Periglac. 13, 259-269.

Shipboard Scientific Party, 1995. Site 911, In: Myhre, A.M., Thiede, J., Firth, J. (Eds.), Proceedings of the Ocean Drilling Program, Initial Reports, Leg 151. Ocean Drilling Program, College Station, TX, pp. 271-318.

Solheim, A., Andersen, E.S., Elverhøi, A., Fiedler, A., 1996. Late Cenozoic depositional history of the western Svalbard continental shelf, controlled by subsidence and climate. Global Planet. Change 12, 135–148.

Svendsen, J. I., Alexanderson, H., Astakhov, V.I., Demidov, I., Dowdeswell, J.A., Funder, S., Gataullin, V., Henriksen, M., Hjort, C., Houmark-Nielsen, M., Hubberten, H., Ingolfsson, O., Jakobsson, M., Kjær, K., Larsen, E., Lokrantz, H., Lunkka, J.P., Lysa, A., Mangerud, J., Matiouchkov, A., Moller, P., Murray, A., Niessen, F., Nikolskaya, O., Polyak, P., Saarnisto, M., Siegert, C., Siegert, M.J., Spielhagen, R.F., Stein, R., 2004. Late Quaternary ice sheet history of northern Eurasia. Quat. Sci. Rev. 23, 1229–1271, doi:10.1016/j.quascirev.2003.12.008.

Stuiver, M., Reimer, P. J., 1986. A computer program for radiocarbon age calibration, Radiocarbon 28, 1022-1030.

Vorren, T.O., Laberg, J.S., Blaume, F., Dowdeswell, J.A., Kenyon, N.H., Mienert, J., Rumohr, J., Werner, F., 1998. The Norwegian-Greenland Sea continental margins: morphology and late quaternary sedimentary processes and environment. Quat. Sci. Rev. 17, 273–302.

Vogt, P.R., Crane, K., Sundvor, E., 1994. Deep Pleistocene iceberg ploughmarks on the Yermak Plateau: sidescan and 3.5 kHz evidence for thick calving ice fronts and a possible marine ice sheet in the Arctic Ocean. Geology 22, 403-406.

Vogt, C., Knies, J., Spielhagen, R.F., Stein, R., 2001. Detailed mineralogical evidence for two nearly identical glacial/deglacial cycles and Atlantic water advection to the Arctic Ocean during the last 90,000 years. Global Planet. Change 31, 23–44.

Wollenburg, I., 2012. Documentation of Sediment Core PS13/140-4, edited by P. R. f. M. Sediments, Alfred Wegener Institute, Bremerhaven.

Woodworth-Lynas, C.M.T., Simms, A., Rendell, C.M., 1985. Iceberg grounding and scouring on the Labrador Continental Shelf. Cold Regions Science and Technology 10, 163-186.

Zamelczyk, K., Rasmussen, T.L., Husum, K., Godtliebsen, F., Hald, M., 2014. Surface water conditions and calcium carbonate preservation in the Fram Strait during marine isotope stage 2, 28.8–15.4 kyr. Paleoceanography 29, 1–12, doi:10.1002/2012PA002448.

Figure Captions

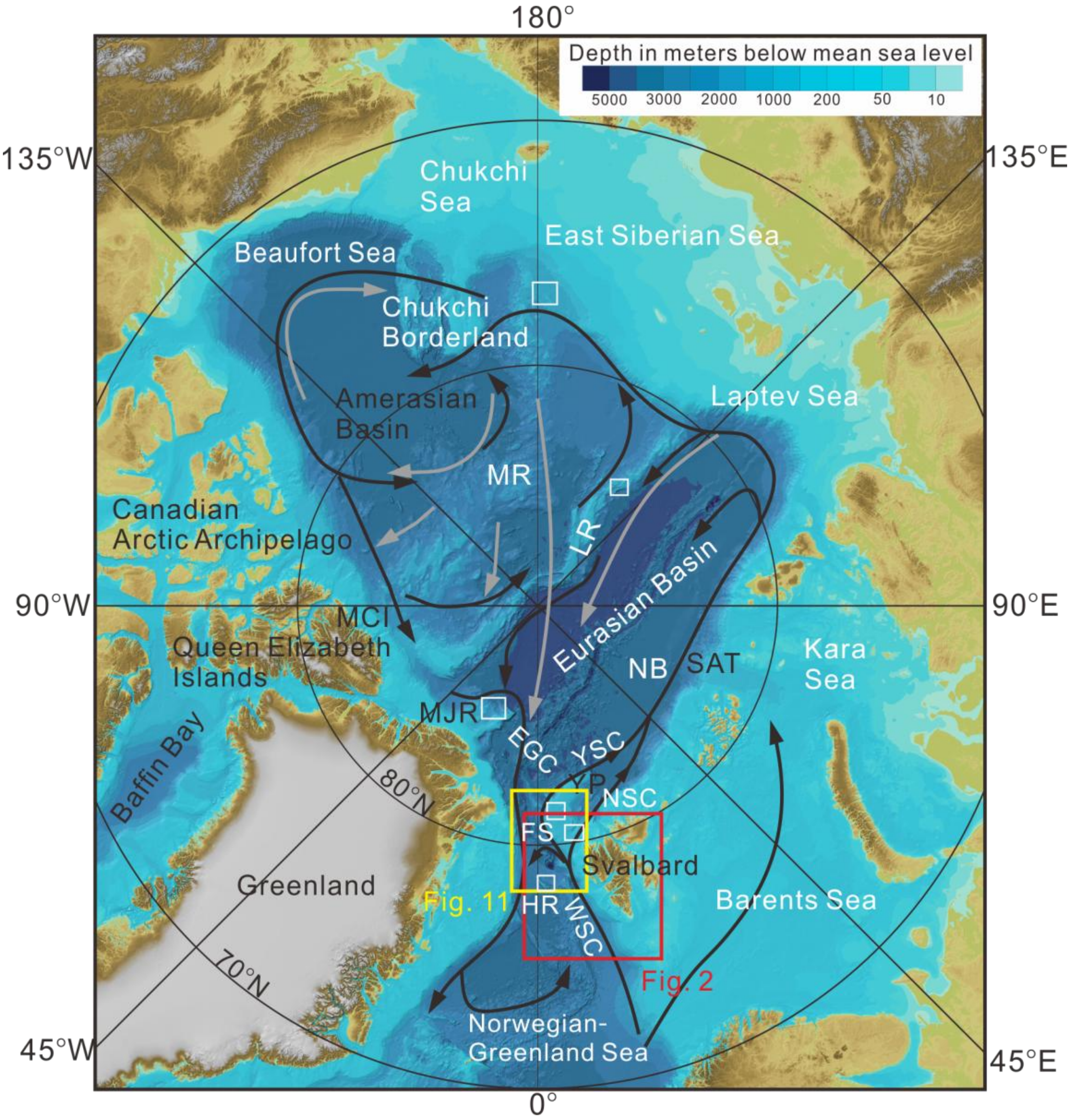

Fig. 1. Bathymetry of the Arctic Ocean (Jakobsson et al., 2012) showing deep iceberg scoured areas and the circulation of surface (gray arrows) and subsurface waters (black arrows). Documented evidence of seafloor erosion by icebergs in previous studies are indicated by white boxes. The boxes mark the locations of Figures 2 and 11. HR, Hovgaard Ridge; FS, Fram Strait; LR, Lomonosov Ridge; MJR, Morris Jesup Rise; MR, Mendeleev Ridge; NB, Nansen Basin; SAT, St Anna Trough; YP, Yermak Plateau; MCI, M' Clintock Inlet; EGC, East Greenland Current; WSC, West Spitsbergen Current; NSC, North Spitsbergen Current; YSC, Yermak Slope Current.

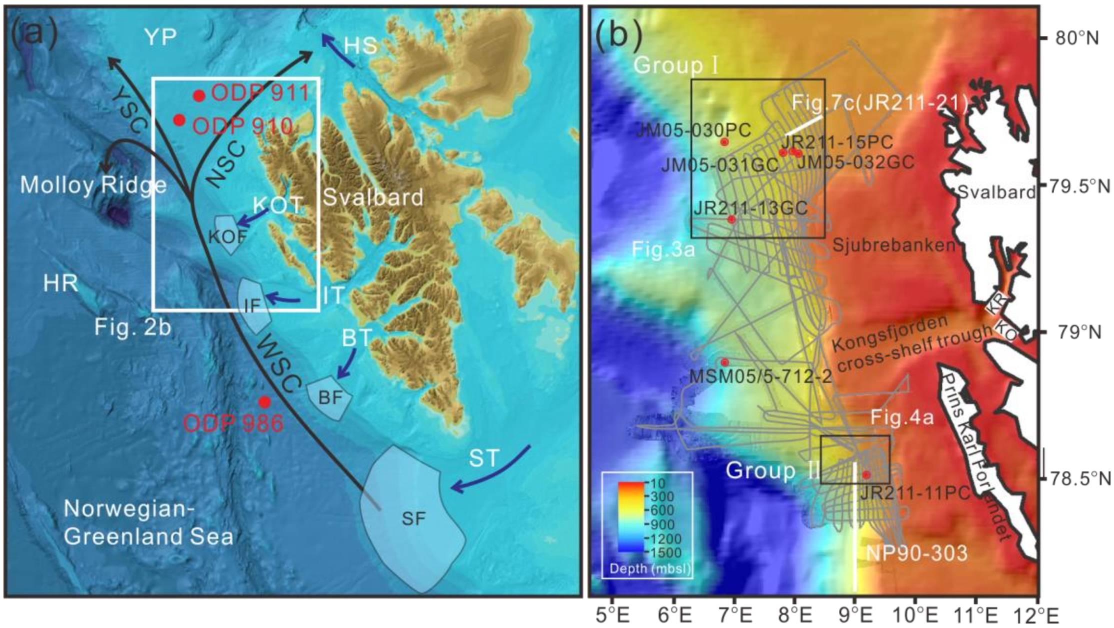

Fig. 2. (a) Overview map of the western Svalbard margin (Jakobsson et al., 2012) showing major cross-shelf troughs and trough-mouth fans. The location of this study area is marked by a white rectangle. (b) Bathymetric Map (Sarkar et al., 2011) showing the survey lines from Cruise JR211. The grey lines indicate the locations of TOPAS sub-bottom profiles. The white lines mark the locations of seismic lines used. NP 90-303 is a published seismic profile along the western Svalbard margin modified from Elverhøi et al. (1995). The locations of figures, sediment cores and ODP sites are labelled in this figure. HS, Hinlopen Strait; KR, Krossfjorden; KO, Kongsfjorden; ST, Storfjorden Trough; SF, Storfjorden Fan; BT, Bellsund Trough; BF, Bellsund Fan; IT, Isfjorden Trough; IF, Isfjorden Fan; KOT, Kongsfjorden Trough; KOF, Kongsfjorden Fan.

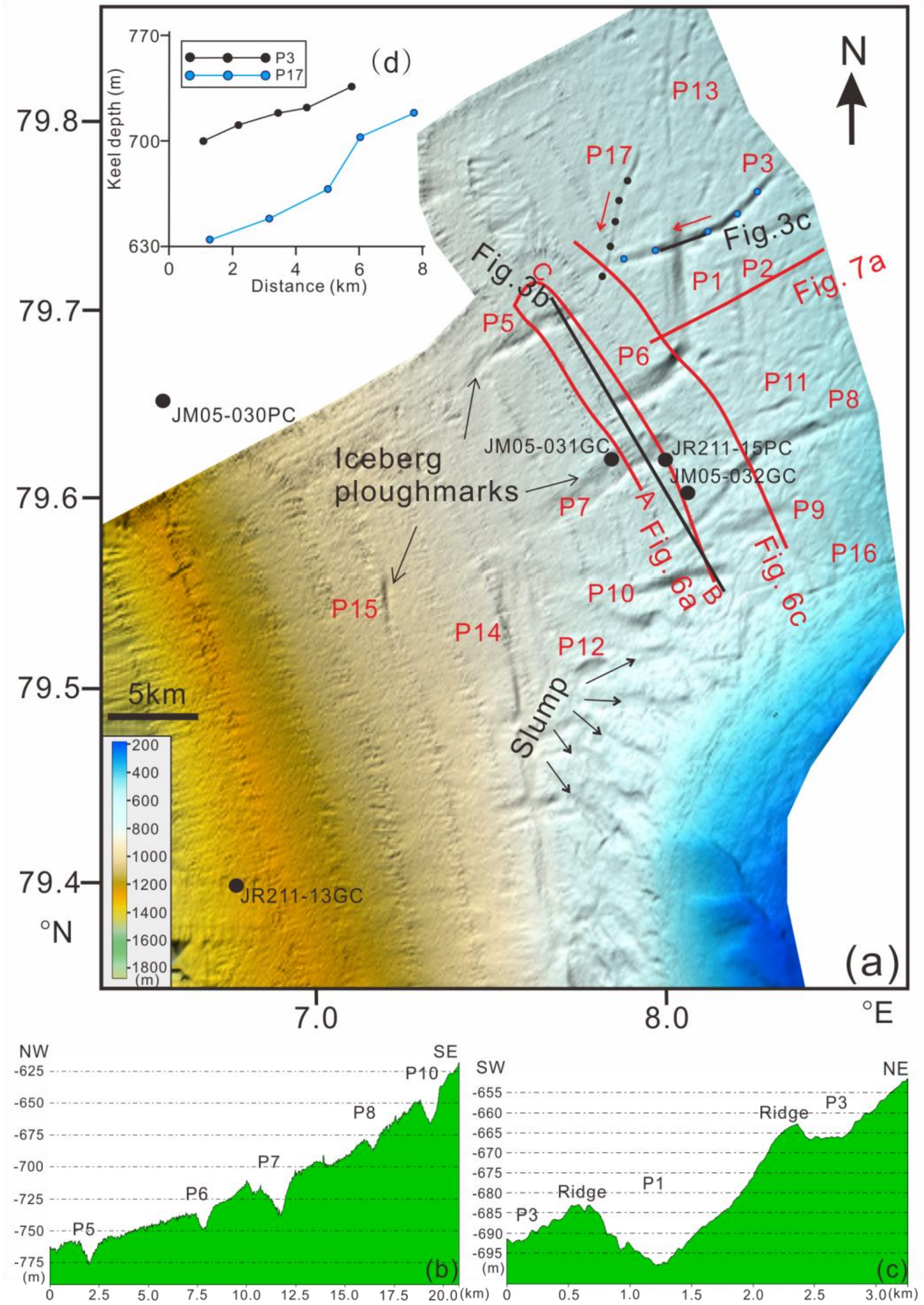

Fig. 3. (a) Bathymetric map of 17 iceberg ploughmarks on northwestern Svalbard margin (Group I). The red solid lines highlight the TOPAS sub-bottom profiles interpreted in this study. The black and blue dots in P3 and P17 correspond to the black and blue dots in Fig. 3d. The red arrows show the measuring direction from SW to NE. (b) Profile showing the geometry of five iceberg scours with a NE-SW orientation. (c) The SW-NE profile illustrating the relationship of P1 and P3. (d) Graph illustrating detailed variation of iceberg ploughmark depth for P3 and P17. Distance is measured along the ploughmark axis and increases to NE.

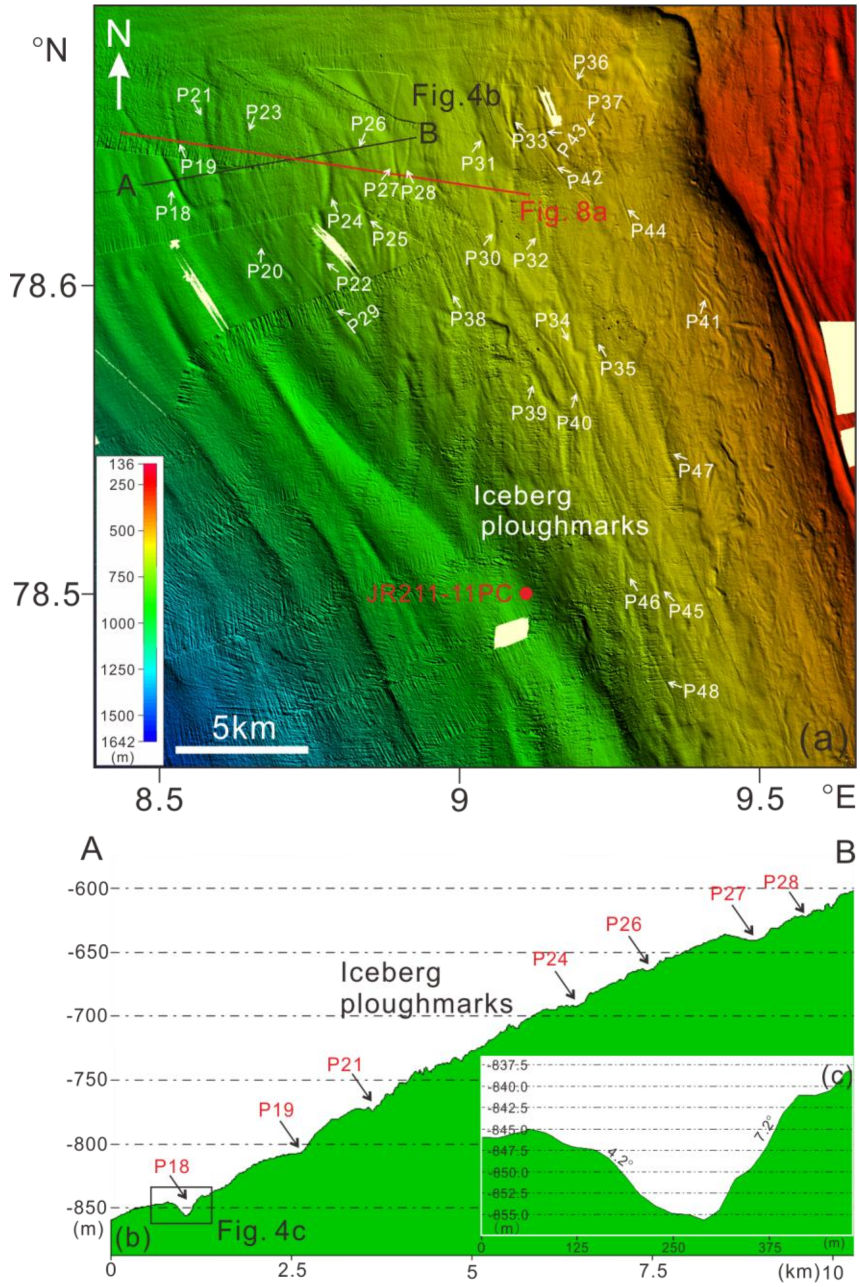

Fig. 4. (a) Detailed morphology of the iceberg ploughmarks identified on western Svalbard margin from bathymetric data (Group II). (b) Profile A-B illustrating the geometry of seven furrows (see location in Fig. 4a). (c) Detailed geometry of a single individual iceberg ploughmark (see location in Fig. 4b). The dip of two flanks are marked.

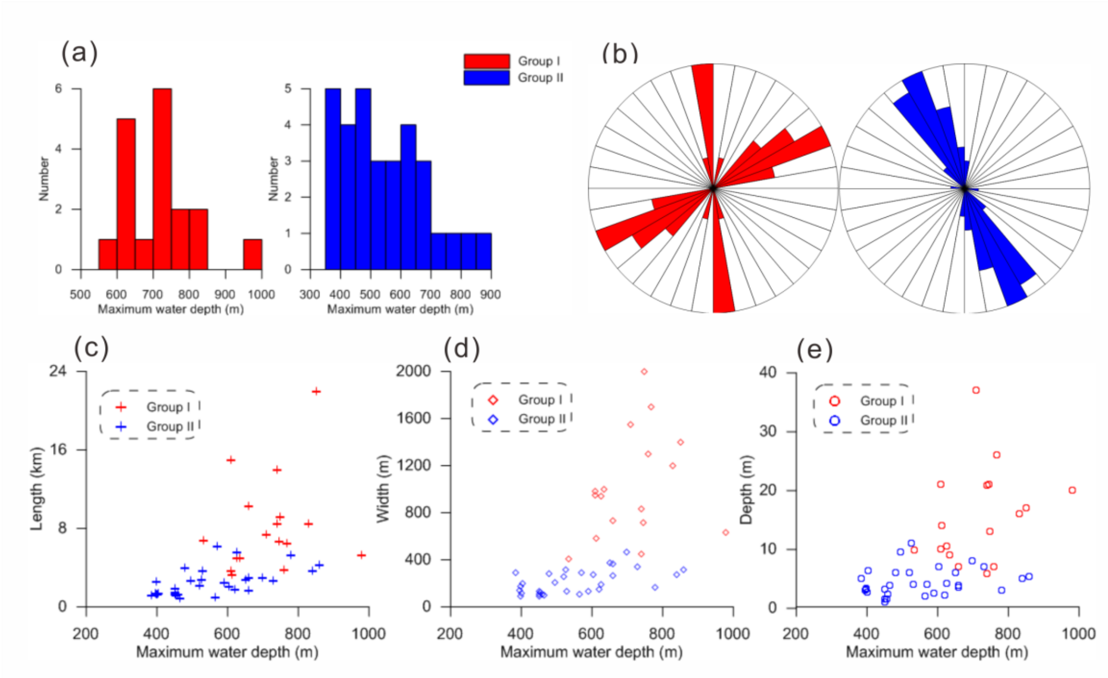

Fig. 5. (a) Bar chart showing the number of iceberg ploughmark in each depth range of the two groups. (b) Rose diagrams showing the orientations of iceberg ploughmarks for each group. Graphs c-e depicting the variations of length, width, depth for the identified iceberg ploughmarks against maximum water depth on the modern seafloor.

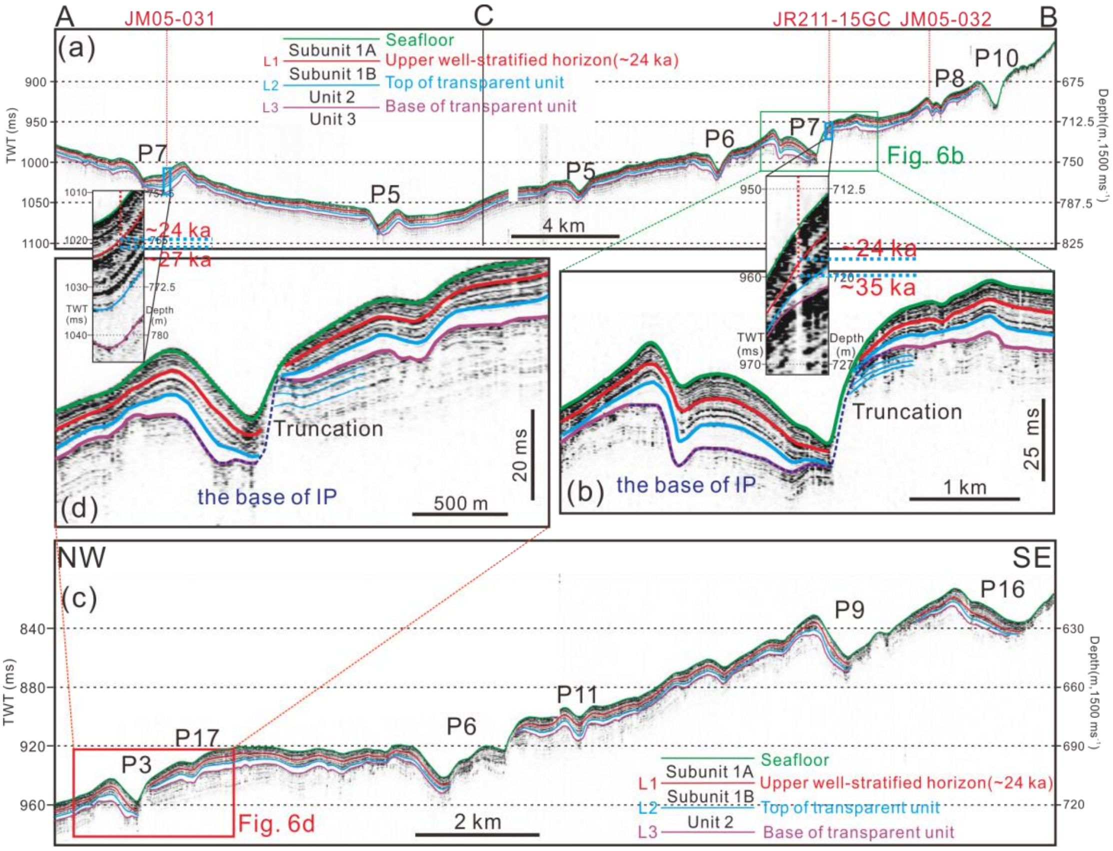

Fig. 6. (a) TOPAS sub-bottom profile on northwestern Svalbard margin (for location see red lines in Fig. 3a) showing five iceberg ploughmarks with SW-NE orientation, three seismic reflectors and three acoustic units (separated by green, blue and purple lines). Three core sites near the line are marked. The radiocarbon dating results of the sediment cores JM05-031 and JR211-15GC have been plotted at L1 and the bottom of these two cores. (b) Zoomed section revealing the base of iceberg ploughmarks and truncated relationship with underlying reflectors. See locations in Fig. 6a. (c) Subbottom profiler data showing another four iceberg ploughmarks of the same age. (d) Enlarged section showing detailed geometry of P3 (see location in Fig. 6c). IP, iceberg ploughmark.

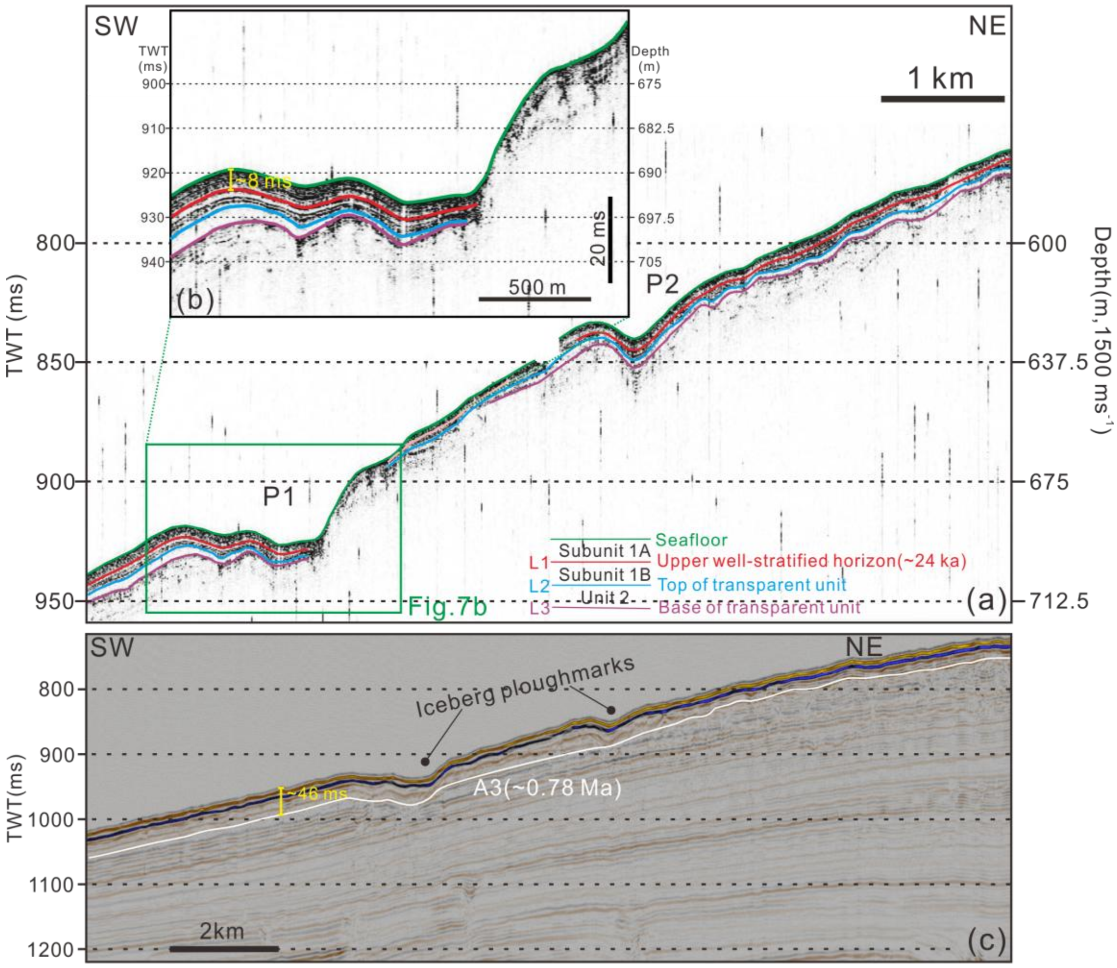

Fig. 7. (a) TOPAS sub-bottom profile (see locations in Fig. 3a) on northwestern Svalbard margin revealing two iceberg ploughmarks in a N-S direction, three seismic reflectors and three acoustic units. (b) Enlarged map of P1 showing the base of IP and truncated the base of Unit 2. (c) The slope-parallel seismic profile JR211-21 showing the published reflector A3 (white; ~0.78 Ma).

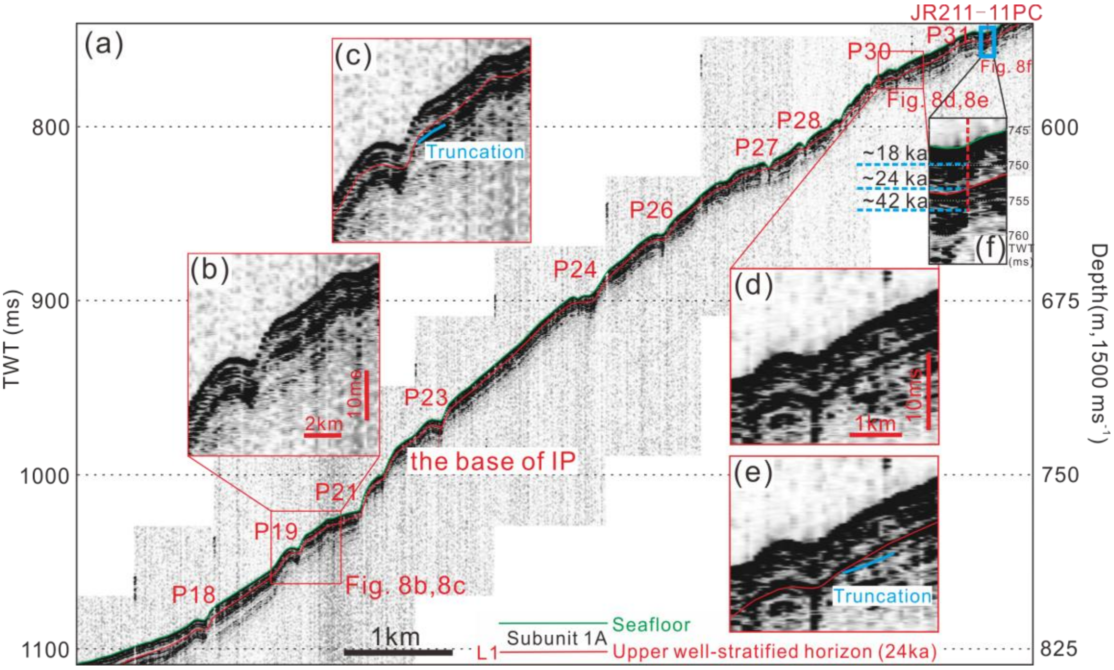

Fig. 8. (a) Sub-bottom profile (see location in Fig. 4a) on the western Svalbard margin showing ten small iceberg ploughmarks. The projection of core JR211-11PC is marked onto the profile. (b-f) Enlarged sections illustrating the shallow acoustic stratigraphy in the area. See location in Fig. 8a.

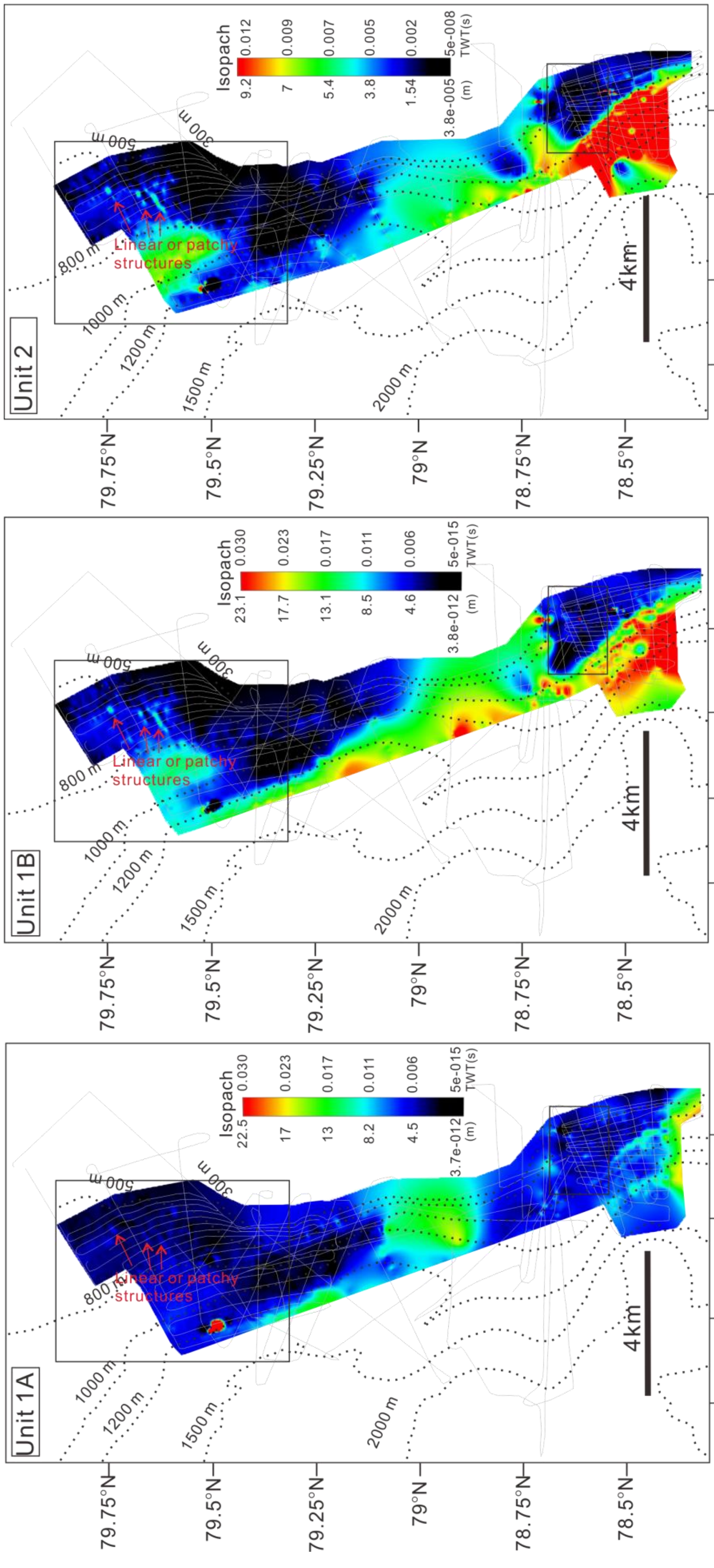
Unit 1A
Unit 1B
Unit 2
Isopach
TWT(s)
(m)
Linear or patchy structures
4km
500 m
300 m
800 m
1000 m
1200 m
1500 m
2000 m
79.75°N
79.5°N
79.25°N
79°N
78.75°N
78.5°N
6°E
7°E
8°E
9°E

Fig. 9. Isopach maps show the variation in sediment thickness (seconds TWT) in stratigraphic units 1A, 1B and 2. The black dotted lines with numbers are contours representing depth below seafloor. The three maps demonstrate similar depositional pattern with increased sediments accumulation on the lower slope compared to sediments starvation on the upper slope.

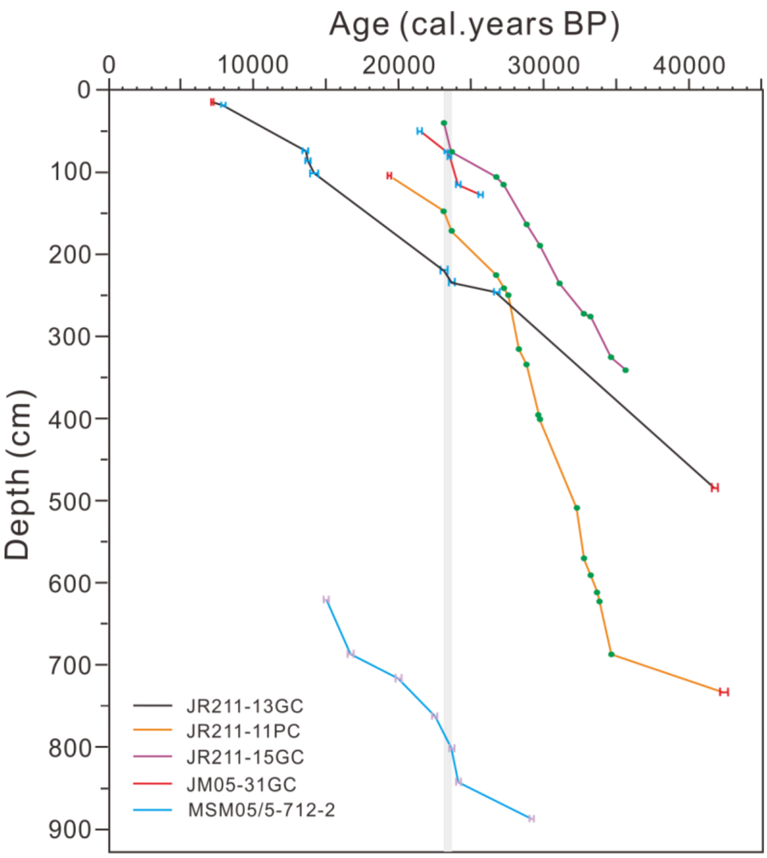

Fig. 10. Age-depth plot of the sediment cores JR211-13GC, JR211-11PC, JR211-15GC, JM05-31GC and MSM05/5-712-2. Age models for cores JM05-31GC and MSM5/5-712-2 are from Jessen et al. (2010) and Zamelczyk et al. (2014), respectively. New radiocarbon ages (with 1 sigma error) are shown in red, magnetic susceptibility tiepoints to the radiocarbon dated stack of Jessen et al. (2010) are shown in blue (error bars indicate 1 sigma error of the calibrated radiocarbon age) and XRF-derived tiepoints from 11PC and 15GC to 13GC are shown in green. A discarded radiocarbon age of 28640 cal yr BP at 363cm depth in 15GC is not plotted here. The vertical grey bar indicates the position of the mass transport deposits.

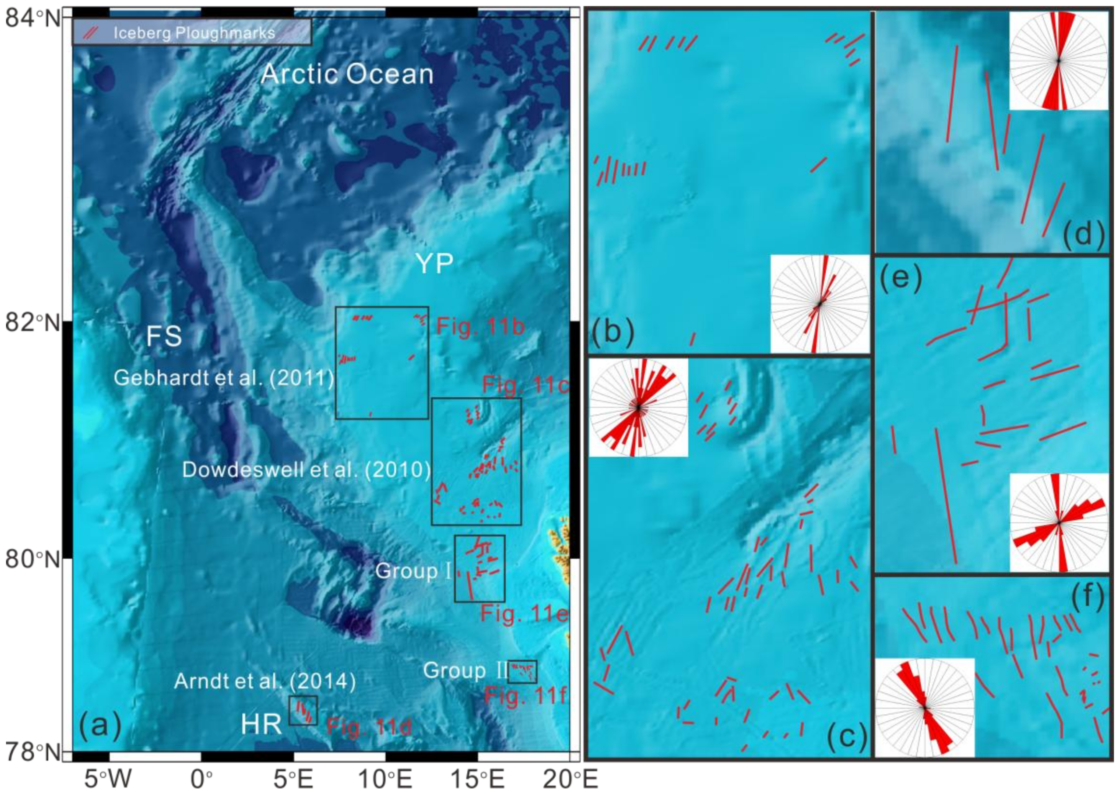

Fig. 11. (a) Map of the distribution of iceberg ploughmarks on the Yermak Plateau, Fram Strait, northwestern Svalbard margin and western Svalbard margin. (b-f) Enlarged map of the black squares in Fig. 11a. Data in subfigures (e) and (f) are from this study.

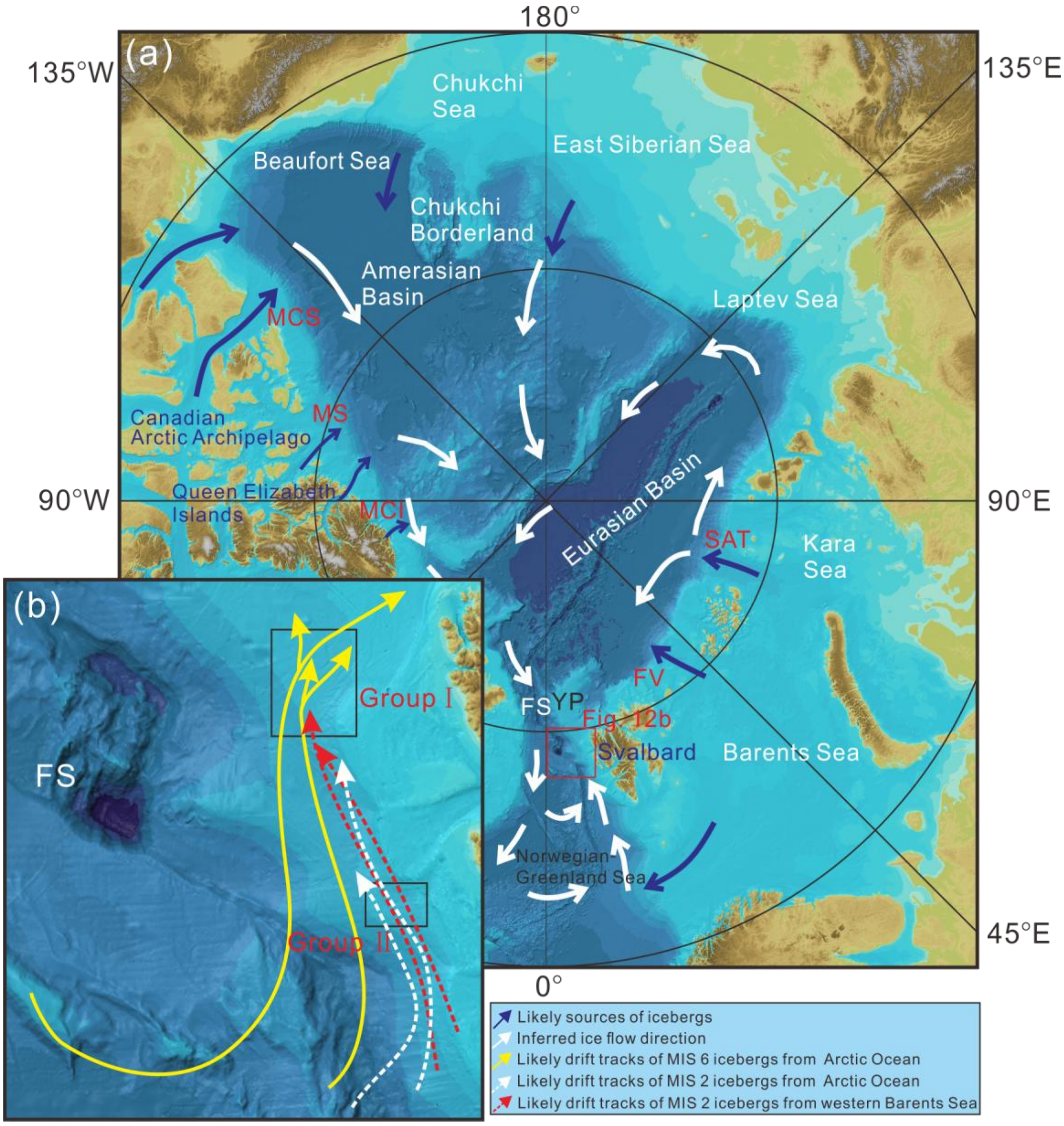

Fig. 12. (a) Inferred ice flow direction indicating the sources of iceberg ploughmarks. Blue arrows indicate fast-flowing ice streams in the troughs and white arrows show paths of transported icebergs from the Arctic Ocean. (b) Enlarged map of the red rectangle in Fig. 12a. The black boxes show the location of observed iceberg ploughmarks on the western Svalbard margin. SAT, St Anna Trough; FV: Franz Victoria; MCI: M’Clintock Inlet; MCS: M’Clure Strait; MS: Massey Sound.

Table 1

Characteristics of three acoustic units on the western Svalbard margin

Acoustic unit	**Reflection characteristics**			**Thickness** TWT(ms)
	Top	**Bottom**	**Internal**	
Unit 1	**Seafloor**: Smooth, continuous wavy	**L2**	Stratified, continuous reflectors, or transparent	~ 2– 40
Subunit 1A	**Seafloor**	**L1**		
Subunit 1B	**L1**: erosional, frequently truncating to base	**L2**		
Unit 2	**L2**: Smooth, continuous wavy	**L3**	Transparent	~1– 12
Unit 3	**L3**: erosional, frequently truncating to base	Not defined	Discontinuous, well-stratified reflections	Not defined